PERGAMON

International Journal of Solids and Structures 38 (2001) 7571–7585

INTERNATIONAL JOURNAL OF SOLIDS and STRUCTURES

www.elsevier.com/locate/ijsolstr

Free vibration of piezoelastic laminated cylindrical shells under hydrostatic pressure

Hongyun Li *, Qirong Lin, Zhengxing Liu, Chao Wang

Department of Engineering Mechanics, Shanghai Jiaotong University, Shanghai 200030, People's Republic of China

Received 9 April 2000

Abstract

Free vibration of piezoelastic laminated cylindrical shells under a hydrostatic pressure is discussed in this paper. From Hamilton's principle nonlinear dynamic equations of the piezoelastic laminated cylindrical shell are derived. Based on which, the dynamic equations of a closed piezoelastic cylindrical shell under a hydrostatic external pressure are obtained. An analytical solution is presented for the case of free vibration of a simply supported piezoelastic laminated cylindrical shell under a hydrostatic pressure, and the influence of fluid–structural coupling effect on the natural frequencies of submerged cylindrical shell is discussed. Numerical results are presented to examine the factors that influence the natural frequencies of the piezoelastic cylindrical shell under a hydrostatic pressure.

Keywords: Piezoelastic cylindrical shell; Free vibration; Hydrostatic pressure; Hamilton's principle

1. Introduction

In recent years, the use of piezoelectric materials in intelligent structures attracted extensive attentions. Due to the intrinsic direct and converse piezoelectric effects, piezoelectric materials can be effectively used as sensors or actuators for the active shape or vibration control of structures. The design of such active systems requires good understanding of the mechanical–electric interaction between the structures and piezoelectric materials. Many investigations have been done on this field (Clinton et al., 1998). However, most of these studies are based on geometrically linear theories (Tzou, 1993). Since many structures like large lightweight space structures or thin-wall vessels can induce large deformations under large external static or dynamic excitations, researches on the induced geometrical nonlinear effects on static and dynamic characteristics of structures are necessary in order to design and control the structural systems effectively.

Baumhauer and Tiersten (1973) developed general piezoelectric nonlinear theory. Pai et al. (1993) proposed a nonlinear model for a composite plate laminated with piezoelectric layers. Yu (1995) provided large deformation equations of piezoelectric plates. Tzou and Bao (1997) presented a geometrical nonlinear

* Corresponding author. Fax: +86-21-62933021.

E-mail address: cmshen@public2.sta.net.cn (H. Li).

PII: S0020-7683(01)00008-7

theory of a piezothermoelastic laminated shell exposed to mechanical, electric and thermal fields. Tzou and Zhou (1995) investigated the dynamic control of a circular plate with geometrical nonlinearity. Nonlinear piezoelectric beams were discussed by Donatus et al. (1998) and Bao et al. (1998).

Stability problem of flexible or thin-wall structures is a primary concern of researchers. However, publication about the stability of piezoelectric structures is few. Chen and Shen (1997) studied the buckling of piezoelectric cylindrical shells of infinite length subjected to external pressure and electric field. No research on stability of finite piezoelectric cylindrical shells has been found by the authors.

In this paper, free vibration of piezoelastic laminated cylindrical shells under hydrostatic pressure is discussed. In Section 2, nonlinear dynamic equations of the piezoelastic laminated cylindrical shell are derived from Hamilton's principle. Then, the dynamic equations of a closed piezoelastic cylindrical shell under a hydrostatic external pressure are obtained in Section 3. In Section 4, an analytical solution is presented for the case of free vibration of a simply supported piezoelastic laminated cylindrical shell under a hydrostatic pressure, and the fluid–structural coupling effect on the natural frequencies of submerged shell is discussed. Numerical results are presented in Section 5, and the factors that influence the natural frequencies of the piezoelastic shell under hydrostatic pressure are examined.

2. Nonlinear piezoelastic laminated cylindrical shell theory

The structure studied in this article is a N layers symmetrically laminated circular cylindrical shell (Fig. 1). The curvilinear coordinate system (x_1, x_2, x_3) shown in Fig. 1 is selected, where the x_1 axis is along the axial direction, the x_2 axis is the rotational angle defining the circumferential direction, and the x_3 axis is along the radial direction. The surface defined by $x_3 = 0$ is set on the middle surface of the shell. R is the radius of curvature of the x_2 axis on the middle surface. Therefore, the relations between cylindrical coordinate system (z, θ, r) and (x_1, x_2, x_3) are: $z = x_1$, $\theta = x_2$, $r = x_3 + R$. Each shell lamina can be composed of an orthotropic, piezoelectric or elastic material. The principle material directions are assumed to coincide with the coordinates x_1, x_2 and x_3. The thickness of kth layer is denoted as h_k $(k = 1, 2, \ldots, N)$, the total thickness of the shell is $h = \sum_{k=1}^{N} h_k$. L denotes the length of the shell.

2.1. Constitutive relations

It is assumed that material properties are constant, and the stress and strain relations are linear. The constitutive relationship of orthotropic piezoelectric materials can be written as follows (Tiersten, 1969):

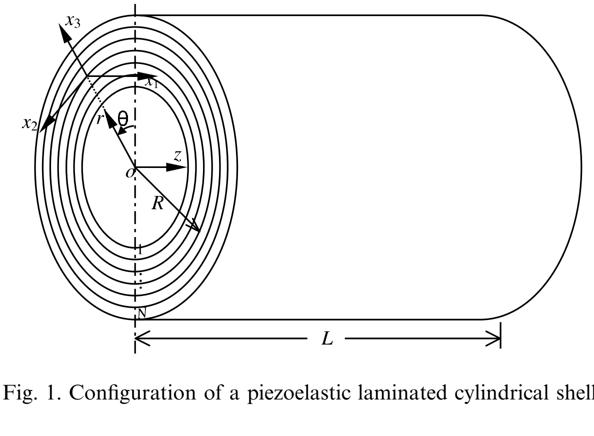

Fig. 1. Configuration of a piezoelastic laminated cylindrical shell.

$$\begin{Bmatrix} \sigma_1 \\ \sigma_2 \\ \sigma_3 \\ \sigma_4 \\ \sigma_5 \\ \sigma_6 \end{Bmatrix} = \begin{bmatrix} c_{11} & c_{12} & c_{13} & 0 & 0 & 0 \\ c_{12} & c_{22} & c_{23} & 0 & 0 & 0 \\ c_{13} & c_{23} & c_{33} & 0 & 0 & 0 \\ 0 & 0 & 0 & c_{44} & 0 & 0 \\ 0 & 0 & 0 & 0 & c_{55} & 0 \\ 0 & 0 & 0 & 0 & 0 & c_{66} \end{bmatrix} \begin{Bmatrix} S_1 \\ S_2 \\ S_3 \\ S_4 \\ S_5 \\ S_6 \end{Bmatrix} - \begin{bmatrix} 0 & 0 & e_{31} \\ 0 & 0 & e_{32} \\ 0 & 0 & e_{33} \\ 0 & e_{24} & 0 \\ e_{15} & 0 & 0 \\ 0 & 0 & 0 \end{bmatrix} \begin{Bmatrix} E_1 \\ E_2 \\ E_3 \end{Bmatrix} \tag{1}$$

$$\begin{Bmatrix} D_1 \\ D_2 \\ D_3 \end{Bmatrix} = \begin{bmatrix} 0 & 0 & 0 & 0 & e_{15} & 0 \\ 0 & 0 & 0 & e_{24} & 0 & 0 \\ e_{31} & e_{32} & e_{33} & 0 & 0 & 0 \end{bmatrix} \begin{Bmatrix} S_1 \\ S_2 \\ S_3 \\ S_4 \\ S_5 \\ S_6 \end{Bmatrix} + \begin{bmatrix} \varepsilon_{11} & 0 & 0 \\ 0 & \varepsilon_{22} & 0 \\ 0 & 0 & \varepsilon_{33} \end{bmatrix} \begin{Bmatrix} E_1 \\ E_2 \\ E_3 \end{Bmatrix} \tag{2}$$

where σ_i, S_i, D_i, E_i represent the stresses, strains, electric displacements, and electric fields, respectively; c_{ij}, e_{ij}, ε_{ii} denote the elastic stiffness constants, piezoelectric stress constants and dielectric constants, respectively. In this paper, the plane stress approximation is made. Thus, while the labels for c_{ij}, e_{ij}, ε_{ii} are not changed, it is assumed they have been adjusted to accommodate the plane stress approximation in the following discussion.

The relations between the electric fields E_i $(i = 1, 2, 3)$ and the electric potential ϕ in the curvilinear coordinate system (Fig. 1) are defined by

$$E_1 = -\frac{\partial \phi}{\partial x_1}, \qquad E_2 = -\frac{1}{R + x_3}\frac{\partial \phi}{\partial x_2}, \qquad E_3 = -\frac{\partial \phi}{\partial x_3} \tag{3}$$

The electric potential function ϕ^k on the kth layer is written as follows (Mitchell and Reddy, 1995):

$$\phi^k(x_1, x_2, x_3, t) = \sum_{j=1}^{M} f_j^k(x_3)\varphi_j^k(x_1, x_2, t) \quad (k = 1, 2, \ldots, N) \tag{4}$$

where M is the number of interpolation nodes, and $f_j^k(x_3)$ $(j = 1, \ldots, M)$ are Lagrange interpolation functions.

2.2. Nonlinear strain–displacement relations

The nonlinear strain of the structure can be introduced by large deformations, which in turn can be introduced mechanically and/or electrically. According to the Love–Kirchhoff thin shell assumptions, the nonlinear deflection $U_i(x_1, x_2, x_3, t)$ $(i = 1, 2, 3)$ in the ith direction can be expressed as (Tzou, 1993)

$$\begin{aligned} U_1(x_1, x_2, x_3, t) &= u_1(x_1, x_2, t) + \theta_1(x_1, x_2, t)x_3 \\ U_2(x_1, x_2, x_3, t) &= u_2(x_1, x_2, t) + \theta_2(x_1, x_2, t)x_3 \\ U_3(x_1, x_2, x_3, t) &= u_3(x_1, x_2, t) \end{aligned} \tag{5}$$

where $u_i(x_1, x_2, t)$ $(i = 1, 2, 3)$ is the displacement component of a point on the midplane of the shell along the x_i $(i = 1, 2, 3)$ axis; θ_1 and θ_2 represent the rotations of a transverse normal at $x_3 = 0$ about the x_2 and $-x_1$ axes, respectively. The laminated shell is considered to be thin, so that the transverse normal strains S_3 and shear strains S_4, S_5 are negligible. Thus, the rotational angles θ_1 and θ_2 for the thin laminated shell are defined as (Tzou and Bao, 1997):

$$\theta_1 = -\frac{\partial u_3}{\partial x_1}, \qquad \theta_2 = \frac{u_2}{R} - \frac{1}{R}\frac{\partial u_3}{\partial x_2} \tag{6}$$

In general, for a thin shell, the in-plane deflections are much smaller than the transverse deflections. Thus, the nonlinear effects due to the in-plane large deflections are usually neglected (Palazatto and Dennis, 1992), only the nonlinear strains due to the large transverse deflection u_3 are considered. Therefore, the nonlinear strain–displacement relations can be written as:

$$\begin{Bmatrix} S_1 \\ S_2 \\ S_6 \end{Bmatrix} = \begin{Bmatrix} s_1 \\ s_2 \\ s_6 \end{Bmatrix} + x_3 \begin{Bmatrix} \kappa_1 \\ \kappa_2 \\ \kappa_6 \end{Bmatrix} \tag{7}$$

where s_1, s_2, s_6 are the membrane strains, and κ_1, κ_2, κ_6 are the bending strains. Subscripts 1, 2, 6 respectively denote the two normal strains and in-plane shear strain. Detailed membrane and bending strains are written as functions of displacements u_i $(i = 1, 2, 3)$

$$s_1 = \frac{\partial u_1}{\partial x_1} + \frac{1}{2}\left(\frac{\partial u_3}{\partial x_1}\right)^2 \tag{8a}$$

$$s_2 = \frac{1}{R}\frac{\partial u_2}{\partial x_2} + \frac{u_3}{R} + \frac{1}{2}\left(\frac{\partial u_3}{R\,\partial x_2}\right)^2 \tag{8b}$$

$$s_6 = \frac{1}{R}\frac{\partial u_1}{\partial x_2} + \frac{\partial u_2}{\partial x_1} + \frac{1}{R}\frac{\partial u_3}{\partial x_2}\frac{\partial u_3}{\partial x_1} \tag{8c}$$

$$\kappa_1 = -\frac{\partial^2 u_3}{\partial x_1^2}, \qquad \kappa_2 = \frac{\partial u_2}{R^2\,\partial x_2} - \frac{1}{R^2}\frac{\partial^2 u_3}{\partial x_2^2}, \qquad \kappa_6 = \frac{\partial u_2}{R\,\partial x_1} - \frac{2}{R}\frac{\partial^2 u_3}{\partial x_1\,\partial x_2} \tag{8d}$$

2.3. Hamilton's principle and nonlinear system equations

The system equations and boundary conditions of the piezoelastic shell can be derived from Hamilton's principle:

$$\delta \int_{t_0}^{t_1} (T - \Pi)\,\mathrm{d}t = 0 \tag{9}$$

where T is the kinetic energy: $T = \int_V \frac{1}{2}\rho \dot{U}_j \dot{U}_j\,\mathrm{d}V$; Π is the total potential energy: $\Pi = \int_V \hbar(S_i, E_j)\,\mathrm{d}V - \int_A [t_j U_j - Q_j \phi]\,\mathrm{d}A$; $\hbar$ is the electric enthalpy: $\hbar = \frac{1}{2}\{S\}^T[c]\{S\} - \frac{1}{2}\{E\}^T[\varepsilon]\{E\} - \{E\}^T[e]\{S\}$. ρ is the mass density; t_j is the surface traction in the x_j direction, Q_j is the surface electric charge; U_j and $\dot{U}_j$ are the displacement and velocity; V and A are the volume and surface of the piezoelastic shell continuum, respectively. Considering the N layers piezoelastic shell discussed in this paper, Hamilton's equation can be rewritten as follows:

$$\int_{t_0}^{t_1} \sum_{k=1}^{N} \int_{V_k} \frac{1}{2}\rho_k \delta\left(\sum_{j=1}^{3} (\dot{U}_j)^2\right) \mathrm{d}V\,\mathrm{d}t - \int_{t_0}^{t_1} \sum_{k=1}^{N} \int_{V_k} \left(\{\sigma\}_k^T \delta\{S\}_k - \{D\}_k^T \delta\{E\}_k\right) \mathrm{d}V\,\mathrm{d}t + \int_{t_0}^{t_1} \sum_{k=1}^{N} \int_{A_k} (t_j \delta U_j - Q_j \delta\phi)\,\mathrm{d}A\,\mathrm{d}t = 0 \tag{10}$$

Note that membrane force resultants N_i $(i = 1, 2, 6)$ and M_i $(i = 1, 2, 6)$ can be written as:

$$\begin{Bmatrix} N_1 \\ N_2 \\ N_6 \end{Bmatrix} = \int_{-h/2}^{h/2} \begin{Bmatrix} \sigma_1 \\ \sigma_2 \\ \sigma_6 \end{Bmatrix} \mathrm{d}x_3 = \begin{bmatrix} A_{11} & A_{12} & 0 \\ A_{12} & A_{22} & 0 \\ 0 & 0 & A_{66} \end{bmatrix} \begin{Bmatrix} s_1 \\ s_2 \\ s_6 \end{Bmatrix} + \begin{Bmatrix} N_1^{\mathrm{e}} \\ N_2^{\mathrm{e}} \\ N_6^{\mathrm{e}} \end{Bmatrix} \tag{11}$$

$$\begin{Bmatrix} M_1 \\ M_2 \\ M_6 \end{Bmatrix} = \int_{-h/2}^{h/2} x_3 \begin{Bmatrix} \sigma_1 \\ \sigma_2 \\ \sigma_6 \end{Bmatrix} \mathrm{d}x_3 = \begin{bmatrix} B_{11} & B_{12} & 0 \\ B_{12} & B_{22} & 0 \\ 0 & 0 & B_{66} \end{bmatrix} \begin{Bmatrix} \kappa_1 \\ \kappa_2 \\ \kappa_6 \end{Bmatrix} + \begin{Bmatrix} M_1^{\mathrm{e}} \\ M_2^{\mathrm{e}} \\ M_6^{\mathrm{e}} \end{Bmatrix} \tag{12}$$

where superscript e represents the component induced by the electric field. The laminate stiffness A_{ij}, B_{ij} $(i,j = 1,2,6)$ are defined as

$$A_{ij} = \sum_{k=1}^{N} (c_{ij})_k (x_{3_k} - x_{3_{k-1}}), \qquad B_{ij} = \frac{1}{3} \sum_{k=1}^{N} (c_{ij})_k (x_{3_k}^3 - x_{3_{k-1}}^3)$$

where x_{3_k} and $x_{3_{k-1}}$ denote the coordinate values in x_3 axis of the outer and inner surface of the kth layer, respectively. It is assumed that in-plane electric fields E_1 and E_2 are zero in the thin piezoelastic shell laminate, and only the transverse electric field E_3 is considered in the analysis. Thus, the resultants due to the piezoelectric effect can be written as

$$N_1^{\mathrm{e}} = \sum_{k=1}^{N} e_{31}^k \left(\sum_{j=1}^{M} \eta_{jk} \varphi_j^k \right), \qquad N_2^{\mathrm{e}} = \sum_{k=1}^{N} e_{32}^k \left(\sum_{j=1}^{M} \eta_{jk} \varphi_j^k \right), \qquad N_6^{\mathrm{e}} = 0 \tag{13}$$

$$M_1^{\mathrm{e}} = \sum_{k=1}^{N} e_{31}^k \left(\sum_{j=1}^{M} \beta_{jk} \varphi_j^k \right), \qquad M_2^{\mathrm{e}} = \sum_{k=1}^{N} e_{32}^k \left(\sum_{j=1}^{M} \beta_{jk} \varphi_j^k \right), \qquad M_6^{\mathrm{e}} = 0 \tag{14}$$

where

$$\eta_{jk} = \int_{x_{3_{k-1}}}^{x_{3_k}} \frac{\mathrm{d}f_j^k}{\mathrm{d}x_3} \mathrm{d}x_3, \quad \beta_{jk} = \int_{x_{3_{k-1}}}^{x_{3_k}} x_3 \frac{\mathrm{d}f_j^k}{\mathrm{d}x_3} \mathrm{d}x_3 \qquad (j = 1,2,\ldots,M;\ \ k = 1,2,\ldots,N)$$

Considering Eq. (5), the inertia force terms can be rewritten as

$$\int_{-h/2}^{h/2} \rho_k \ddot{U}_j \, \mathrm{d}x_3 = \int_{-h/2}^{h/2} \rho_k (\ddot{u}_j + x_3 \theta_j) \, \mathrm{d}x_3 = \rho_s h \ddot{u}_j \quad (i = 1,2) \tag{15}$$

$$\int_{-h/2}^{h/2} \rho_k \ddot{U}_j x_3 \, \mathrm{d}x_3 = \int_{-h/2}^{h/2} \rho_k (\ddot{u}_j + x_3 \theta_j) x_3 \, \mathrm{d}x_3 = \tilde{B} \ddot{\theta}_j \qquad (i = 1,2) \tag{16}$$

$$\int_{-h/2}^{h/2} \rho_k \ddot{U}_3 \, \mathrm{d}x_3 = \int_{-h/2}^{h/2} \rho_k \ddot{u}_3 \, \mathrm{d}x_3 = \rho_s h \ddot{u}_3 \tag{17}$$

where $\rho_s = (\sum_{k=1}^{N} \rho_k h_k)/h$ is defined as a weight average density for the multi-layered shell and $\tilde{B} = \frac{1}{3} \sum_{k=1}^{N} \rho_k (x_{3_k}^3 - x_{3_{k-1}}^3)$. The effect of rotatory inertia $\tilde{B}\ddot{\theta}_j$ can be neglected in the thin laminated shells without large rotational effect. Therefore, one can derive the nonlinear piezoelastic shell equations and boundary conditions from Eq. (10).

$$\frac{\partial N_1}{\partial x_1} + \frac{\partial N_6}{R \, \partial x_2} = \rho_s h \ddot{u}_1 \tag{18}$$

$$\frac{\partial N_2}{R\,\partial x_2} + \frac{\partial N_6}{\partial x_1} + \frac{F_2}{R} = \rho_s h \ddot{u}_2 \tag{19}$$

$$\frac{\partial F_1}{\partial x_1} + \frac{1}{R}\frac{\partial F_2}{\partial x_2} - \frac{N_2}{R} + \left\{ \frac{\partial}{\partial x_1}\left(N_1 \frac{\partial u_3}{\partial x_1}\right) + \frac{1}{R^2}\frac{\partial}{\partial}\left(N_2 \frac{\partial u_3}{\partial x_2}\right) + \frac{1}{R}\frac{\partial N_6}{\partial x_1}\frac{\partial u_3}{\partial x_2} + \frac{1}{R}\frac{\partial N_6}{\partial x_2}\frac{\partial u_3}{\partial x_1} + \frac{2}{R} N_6 \frac{\partial^2 u_3}{\partial x_1 \partial x_2} \right\} + \sum_{k=1}^{N} \sigma_3\Big|_{x_{3_{k-1}}}^{x_{3_k}} = \rho_s h \ddot{u}_3 \tag{20}$$

where

$$F_1 = \frac{\partial M_1}{\partial x_1} + \frac{\partial M_6}{R\,\partial x_2}, \qquad F_2 = \frac{\partial M_2}{R\,\partial x_2} + \frac{\partial M_6}{\partial x_1}$$

Eqs. (18)–(20) coincide with Eqs. (23)–(25) (Tzou and Bao, 1997) when $R_1 = \infty$, $R_2 = R$, $A_1 = 1$, $A_2 = R$. All terms inside the brace of Eq. (20) are contributed by geometric nonlinear effect. Eqs. (18)–(20) look like equations for a elastic shell. However, from Eqs. (11) and (12), it can be seen that the force and moment resultants are defined by mechanical and electric effects, which are more complicated than the conventional elastic expressions. Admissible mechanical boundary conditions are:

(a) Boundary surfaces which are normal to x_1 axis:

$$N_1^0 \text{ or } u_1^0, \quad M_1^0 \text{ or } \theta_1^0, \quad N_6^0 + \frac{M_6^0}{R} \text{ or } u_2^0$$

$$F_1^0 + \frac{\partial M_6^0}{R\,\partial x_2} + \left[N_1 \frac{\partial u_3}{\partial x_1} + \frac{N_6}{R}\frac{\partial u_3}{\partial x_2}\right]^0 \text{ or } u_3^0$$

(b) Boundary surfaces which are normal to x_2 axis:

$$N_2^0 \text{ or } u_2^0, \quad M_2^0 \text{ or } \theta_2^0, \quad N_6^0 \text{ or } u_1^0$$

$$F_2^0 + \frac{\partial M_6^0}{\partial x_1} + \left[\frac{N_2}{R}\frac{\partial u_3}{\partial x_2} + N_6 \frac{\partial u_3}{\partial x_1}\right]^0 \text{ or } u_3^0$$

Superscript 0 denotes the given physical boundary condition.

For sensor purposes, there exist two conditions for piezoelectric laminae: one is the close circuit (Lee, 1990), and the other is the open circuit (Tzou et al., 1993). For the piezoelectric layer in the close circuit condition, the potentials on the surfaces of the laminae are specified. In this paper, the piezoelectric layer is in the open circuit condition, the charge equation is

$$D_3^{jk} = \int_{x_{3_{k-1}}}^{x_{3_k}} D_3 \frac{\mathrm{d}f_j^k}{\mathrm{d}x_3}\,\mathrm{d}x_3 = 0 \tag{21}$$

Electric boundary conditions on the transverse surface S_{3_k} in the open circuit condition are

$$D_{3_k} + Q_{3_k}^0 = 0 \quad (k = 0, 1, 2, \ldots, N) \tag{22}$$

$Q_{3_k}^0$ is the external charge density on the kth surface.

3. Dynamic equations of closed piezoelastic cylindrical shells under hydrostatic external pressure

The dynamic characteristics of a closed piezoelastic cylindrical shell under hydrostatic pressure are discussed in this section. It is assumed that the shell is subjected to a hydrostatic external pressure q and a radial dynamic pressure $P_1(x_1, x_2, t)$ on its outer surface. Assuming (U_{10}, U_{20}, U_{30}) are the displacements of the shell under the hydrostatic pressure, $(\overline{U}_1, \overline{U}_2, \overline{U}_3)$ are small deflections deviating from (U_{10}, U_{20}, U_{30}) due to the disturbing force $P_1(x_1, x_2, t)$. Hence, the displacements of the shell can be expressed as:

$$U_i \rightarrow U_{i0} + \overline{U}_i \quad (i = 1, 2, 3) \tag{23}$$

Also, force and moment resultants can be expressed as

$$N_i \rightarrow N_{i0} + \overline{N}_i, \quad M_i \rightarrow M_{i0} + \overline{M}_i \qquad (i = 1, 2, 6) \tag{24}$$

Therefore, substituting Eqs. (23) and (24) into Eqs. (18)–(20), and considering $N_{10} = (-qR/2)$, $N_{20} = -qR$, $N_{60} = 0$ at the same time, after eliminating all terms denoted by subscript 0 and omitting the high order terms denoted by superscript '–' and the terms including $\partial U_{30}/\partial x_1$ or $\partial U_{30}/\partial x_2$, the dynamic equations of the piezoelastic circular cylindrical shell under hydrostatic external pressure are written as:

$$\frac{\partial \overline{N}_1}{\partial x_1} + \frac{\partial \overline{N}_6}{R\,\partial x_2} = \rho_s h \ddot{\overline{u}}_1 \tag{25}$$

$$\frac{\partial \overline{N}_2}{R\,\partial x_2} + \frac{\partial \overline{N}_6}{\partial x_1} + \frac{1}{R}\left(\frac{\partial \overline{M}_2}{R\,\partial x_2} + \frac{\partial \overline{M}_6}{\partial x_1}\right) = \rho_s h \ddot{\overline{u}}_2 \tag{26}$$

$$\frac{\partial}{\partial x_1}\left(\frac{\partial \overline{M}_1}{\partial x_1} + \frac{\partial \overline{M}_6}{R\,\partial x_2}\right) + \frac{1}{R}\frac{\partial}{\partial x_2}\left(\frac{\partial \overline{M}_2}{R\,\partial x_2} + \frac{\partial \overline{M}_6}{\partial x_1}\right) - \frac{\overline{N}_2}{R} - \frac{qR}{2}\frac{\partial^2 \overline{u}_3}{\partial x_1^2} - \frac{q}{R}\frac{\partial^2 \overline{u}_3}{\partial x_2^2} - P_1 = \rho_s h \ddot{\overline{u}}_3 \tag{27}$$

Similarly, the electric displacement equilibrium equation (21) can be rewritten as

$$\overline{D}_3^{jk} = 0 \quad (j = 1, 2, \ldots, M, \; k = 1, 2, \ldots, N) \tag{28}$$

Also neglecting the terms including $\partial U_{30}/\partial x_1$ and $\partial U_{30}/\partial x_2$ from Eq. (8), we obtain

$$\overline{s}_1 = \frac{\partial \overline{u}_1}{\partial x_1}, \qquad \overline{s}_2 = \frac{1}{R}\frac{\partial \overline{u}_2}{\partial x_2} + \frac{\overline{u}_3}{R}, \qquad \overline{s}_6 = \frac{1}{R}\frac{\partial \overline{u}_1}{\partial x_2} + \frac{\partial \overline{u}_2}{\partial x_1} \tag{29a}$$

$$\overline{\kappa}_1 = -\frac{\partial^2 \overline{u}_3}{\partial x_1^2}, \qquad \overline{\kappa}_2 = \frac{\partial \overline{u}_2}{R^2\,\partial x_2} - \frac{1}{R^2}\frac{\partial^2 \overline{u}_3}{\partial x_2^2}, \qquad \overline{\kappa}_6 = \frac{\partial \overline{u}_2}{R\,\partial x_1} - \frac{2}{R}\frac{\partial^2 \overline{u}_3}{\partial x_1\,\partial x_2} \tag{29b}$$

Substituting Eqs. (13), (14) and (29) into Eqs. (11) and (12) yields

$$
\begin{aligned}
\overline{N}_1 &= A_{11}\frac{\partial \overline{u}_1}{\partial x_1} + A_{12}\left(\frac{\partial \overline{u}_2}{R\,\partial x_2} + \frac{\overline{u}_3}{R}\right) + \sum_{k=1}^{N} e_{31}^k \left(\sum_{j=1}^{M} \eta_{jk}\overline{\varphi}_j^k\right) \\
\overline{N}_2 &= A_{12}\frac{\partial \overline{u}_1}{\partial x_1} + A_{22}\left(\frac{\partial \overline{u}_2}{R\,\partial x_2} + \frac{\overline{u}_3}{R}\right) + \sum_{k=1}^{N} e_{32}^k \left(\sum_{j=1}^{M} \eta_{jk}\overline{\varphi}_j^k\right) \\
\overline{N}_6 &= A_{66}\left(\frac{\partial \overline{u}_2}{\partial x_1} + \frac{\partial \overline{u}_1}{R\,\partial x_2}\right) \\
\overline{M}_1 &= -B_{11}\frac{\partial^2 \overline{u}_3}{\partial x_1^2} + B_{12}\left(\frac{\partial \overline{u}_2}{R^2\,\partial x_2} - \frac{\partial^2 \overline{u}_3}{R^2\,\partial x_2^2}\right) + \sum_{k=1}^{N} e_{31}^k \left(\sum_{j=1}^{M} \beta_{jk}\overline{\varphi}_j^k\right) \\
\overline{M}_2 &= -B_{12}\frac{\partial^2 \overline{u}_3}{\partial x_1^2} + B_{22}\left(\frac{\partial \overline{u}_2}{R^2\,\partial x_2} - \frac{\partial^2 \overline{u}_3}{R^2\,\partial x_2^2}\right) + \sum_{k=1}^{N} e_{32}^k \left(\sum_{j=1}^{M} \beta_{jk}\overline{\varphi}_j^k\right) \\
\overline{M}_6 &= B_{66}\left(\frac{\partial \overline{u}_2}{R\,\partial x_1} - \frac{2}{R}\frac{\partial^2 \overline{u}_3}{\partial x_1\,\partial x_2}\right)
\end{aligned}
\tag{30}
$$

Because our concern is the disturbing solutions of the shell under hydrostatic pressure, for simplicity, superscript '–' is omitted from the disturbing variables in following discussions, i.e. $\overline{u}_i$ is expressed by u_i. Substituting Eq. (30) into Eqs. (25)–(27), the equations of motion in terms of displacements and potentials can be derived to be:

$$
A_{11}\frac{\partial^2 u_1}{\partial x_1^2} + A_{66}\frac{\partial^2 u_1}{R^2\,\partial x_2^2} + (A_{12}+A_{66})\frac{\partial^2 u_2}{R\,\partial x_1\,\partial x_2} + A_{12}\frac{\partial u_3}{R\,\partial x_1} + \sum_{k=1}^{N} e_{31}^k\left(\sum_{j=1}^{M}\eta_{jk}\frac{\partial \varphi_j^k}{\partial x_1}\right) = \rho_s h\ddot{u}_1 \tag{31}
$$

$$
\begin{aligned}
&(A_{12}+A_{66})\frac{\partial^2 u_1}{R\,\partial x_1\,\partial x_2} + \left(\frac{A_{22}}{R^2}+\frac{B_{22}}{R^4}\right)\frac{\partial^2 u_2}{\partial x_2^2} + \left(A_{66}+\frac{B_{66}}{R^2}\right)\frac{\partial^2 u_2}{\partial x_1^2} + A_{22}\frac{\partial u_3}{R^2\,\partial x_2} - B_{22}\frac{\partial^3 u_3}{R^4\,\partial x_2^3} \\
&\quad - (B_{12}+2B_{66})\frac{\partial^3 u_3}{R^2\,\partial x_1^2\,\partial x_2} + \frac{1}{R^2}\sum_{k=1}^{N} e_{32}^k\left(\sum_{j=1}^{M}\beta_{jk}\frac{\partial \varphi_j^k}{\partial x_2}\right) + \frac{1}{R}\sum_{k=1}^{N} e_{32}^k\left(\sum_{j=1}^{M}\eta_{jk}\frac{\partial \varphi_j^k}{\partial x_2}\right) = \rho_s h\ddot{u}_2
\end{aligned}
\tag{32}
$$

$$
\begin{aligned}
&-A_{12}\frac{\partial u_1}{R\,\partial x_1} - A_{22}\frac{\partial u_2}{R^2\,\partial x_2} + (2B_{66}+B_{12})\frac{\partial^3 u_2}{R^2\,\partial x_1^2\,\partial x_2} + B_{22}\frac{\partial^3 u_2}{R^4\,\partial x_2^3} - A_{22}\frac{u_3}{R^2} - B_{11}\frac{\partial^4 u_3}{\partial x_1^4} - 2(B_{12}+2B_{66}) \\
&\quad \times \frac{\partial^4 u_3}{R^2\,\partial x_1^2\,\partial x_2^2} - B_{22}\frac{\partial^4 u_3}{R^4\,\partial x_2^4} - \frac{qR}{2}\frac{\partial^2 u_3}{\partial x_1^2} - q\frac{\partial^2 u_3}{R\,\partial x_2^2} - P_1 - \frac{1}{R}\sum_{k=1}^{N} e_{32}^k\left(\sum_{j=1}^{M}\eta_{jk}\varphi_j^k\right) \\
&\quad + \sum_{k=1}^{N} e_{31}^k\left(\sum_{j=1}^{M}\beta_{jk}\frac{\partial^2 \varphi_j^k}{\partial x_1^2}\right) + \frac{1}{R^2}\sum_{k=1}^{N} e_{32}^k\left(\sum_{j=1}^{M}\beta_{jk}\frac{\partial^2 \varphi_j^k}{\partial x_2^2}\right) = \rho_s h\ddot{u}_3
\end{aligned}
\tag{33}
$$

The electric displacement equilibrium equation expressed by displacements and potentials can be obtained when Eqs. (29a), (29b) and (2) are substituted into Eq. (28):

$$
\begin{aligned}
D_3^{jk} = \int_{x_{3_{k-1}}}^{x_{3_k}} &\left\{ e_{31}^k\frac{\partial u_1}{\partial x_1} + e_{32}^k\left(1+\frac{x_3}{R}\right)\frac{\partial u_2}{R\,\partial x_2} + e_{32}^k\frac{u_3}{R} - x_3\left(e_{31}^k\frac{\partial^2 u_3}{\partial x_1^2} + e_{32}^k\frac{\partial^2 u_3}{R^2\,\partial x_2^2}\right)\right. \\
&\left. - \varepsilon_{33}\left(\sum_{l=1}^{M}\frac{\mathrm{d}f_l^k}{\mathrm{d}x_3}\varphi_l^k\right)\right\}\frac{\mathrm{d}f_j^k}{\mathrm{d}x_3}\,\mathrm{d}x_3 = 0
\end{aligned}
\tag{34}
$$

4. Undamped vibration of a simply supported cylindrical shell

To obtain meaningful solutions, a laminated circular cylindrical shell with simply supported boundary conditions is studied. The composite piezoelastic laminated shell is a hybrid laminate with two piezoelectric layers added symmetrically to a symmetrically laminated elastic shell. The simply supported boundary conditions are:

$$x_1 = 0, L, \qquad N_1 = u_2 = u_3 = \frac{\partial^2 u_3}{\partial x_1^2} = 0 \tag{35}$$

Using the method analogous to Mitchell and Reddy (1995), each piezoelectric layer is regarded as two mathematical layers with equal thickness, whose electric potential can be modeled using linear Lagrange elements. For the free vibration problem of the shell, the electric potentials can be written as:

$$\varphi_1^1 = 0, \qquad \varphi_2^1 = \varphi_1^2 = \varphi_{\mathrm{I}}, \qquad \varphi_2^2 = 0$$

$$\varphi_1^3 = 0, \qquad \varphi_2^3 = \varphi_1^4 = \varphi_{\mathrm{O}}, \qquad \varphi_2^4 = 0$$

where, superscripts ‘1’ and ‘2’ mean the inner and outer parts of the piezoelectric layer on the inner surface of the shell, respectively; superscripts ‘3’ and ‘4’ mean the inner and outer parts of the piezoelectric layer on the outer surface of the shell, respectively. The subscript ‘1’ and ‘2’ denote the inner and outer surfaces of the corresponding layer, respectively.

The solutions satisfying the boundary conditions (35) have the following expressions:

$$\begin{aligned}
u_1 &= u_{mn} \cos(z_m x_1) \cos(n x_2) e^{i\omega t} \\
u_2 &= v_{mn} \sin(z_m x_1) \sin(n x_2) e^{i\omega t} \\
u_3 &= w_{mn} \sin(z_m x_1) \cos(n x_2) e^{i\omega t} \\
\varphi_{\mathrm{I}} &= \varphi_{\mathrm{I}\,mn} \sin(z_m x_1) \cos(n x_2) e^{i\omega t} \\
\varphi_{\mathrm{O}} &= \varphi_{\mathrm{O}\,mn} \sin(z_m x_1) \cos(n x_2) e^{i\omega t}
\end{aligned} \tag{36}$$

where ω is the natural frequency of the cylindrical shell, $z_m = m\pi/L$, m and $2n$ indicate, respectively, the number of half waves in the axial and circumferential directions.

Also, the radial pressure P_1 can be expressed as

$$P_1 = P_{1\,mn} \sin(z_m x_1) \cos(n x_2) e^{i\omega t} \tag{37}$$

Substituting Eqs. (36) and (37) into Eqs. (31)–(34) yields:

$$([H] - q[J])\{V\} = \omega^2 [M]\{V\} + \{T\} \tag{38}$$

in which

$$\{V\} = \{u_{mn}, v_{mn}, w_{mn}, \varphi_{\mathrm{I}\,mn}, \varphi_{\mathrm{O}\,mn}\}^{\mathrm{T}}, \qquad \{T\} = \{0, 0, -P_{1\,mn}, 0, 0\}^{\mathrm{T}}$$

and $[H]$ is a symmetric matrix, whose elements are given by

$$H_{11} = A_{11} z_m^2 + A_{66} \frac{n^2}{R^2}, \qquad H_{12} = -\left(\frac{A_{12} + A_{66}}{R}\right) z_m n, \qquad H_{13} = -\frac{A_{12} z_m}{R}, \qquad H_{14} = H_{15} = 0,$$

$$H_{22} = \left(A_{66} + \frac{B_{66}}{R^2}\right) z_m^2 + \left(A_{22} + \frac{B_{22}}{R^2}\right) \frac{n^2}{R^2}, \qquad H_{23} = \frac{B_{22} n^3}{R^4} + \frac{A_{22} n}{R^2} + (B_{12} + 2B_{66}) \frac{n z_m^2}{R^2},$$

$$H_{24} = \frac{e_{32}n}{R^2}(\beta_{21} + \beta_{12}), \qquad H_{25} = \frac{e_{32}n}{R^2}(\beta_{23} + \beta_{14}),$$

$$H_{33} = B_{11}z_m^4 + 2(B_{12} + 2B_{66})\frac{n^2 z_m^2}{R^2} + \frac{B_{22}n^4}{R^4} + \frac{A_{22}}{R^2},$$

$$H_{34} = (\beta_{21} + \beta_{12})\left(e_{31}z_m^2 + \frac{e_{32}n^2}{R^2}\right), \qquad H_{35} = (\beta_{23} + \beta_{14})\left(e_{31}z_m^2 + \frac{e_{32}n^2}{R^2}\right),$$

$$H_{44} = -\varepsilon_{33}\left(\alpha_1^{22} + \alpha_2^{11}\right), \qquad H_{45} = 0, \qquad H_{55} = -\varepsilon_{33}\left(\alpha_3^{22} + \alpha_4^{11}\right)$$

where

$$\alpha_k^{ij} = \int_{x_{3_{k-1}}}^{x_{3_k}} \frac{\mathrm{d}f_i^k}{\mathrm{d}x_3}\frac{\mathrm{d}f_j^k}{\mathrm{d}x_3}\,\mathrm{d}x_3$$

$[J]$ and $[M]$ are diagonal matrices whose elements are

$$J_{33} = \frac{Rz_m^2}{2} + \frac{n^2}{R}, \quad J_{ii} = 0 \ \ (i = 1, 2, 4, 5), \qquad M_{11} = M_{22} = M_{33} = \rho_s h, \quad M_{44} = M_{55} = 0$$

It can be seen that, from the elements of matrix $[H]$, the dynamic characteristics of a piezoelastic laminated shell is determined not only by the stiffness and mass of the shell but also by the piezoelectric and dielectric coefficients of the piezoelectric layers.

When the hydrostatic external pressure exceeds certain value, the shell may lose stability. Therefore, the investigation of the free vibration of the cylindrical shell under hydrostatic pressure is meaningful only when the hydrostatic pressure is below the critical hydrostatic pressure q_{cr}. The critical hydrostatic pressure q_{cr} can be obtained when the determinant of the coefficient matrix of the left-hand side of Eq. (38) vanishes, i.e. $|[H] - q_{\mathrm{cr}}[J]| = 0$.

4.1. Free vibration of a piezoelastic cylindrical shell under hydrostatic pressure

Neglecting the coupling effect of the fluid and structure, one can obtain the frequency equation as follows with P_{1mn} removed from Eq. (38):

$$([H] - sq_{\mathrm{cr}}[J])\{V\} = \omega^2[M]\{V\} \tag{39}$$

in which, s denotes the ratio of hydrostatic pressure q to critical pressure q_{cr}. From Eq. (39), the effect of hydrostatic pressure on the natural frequencies of the circular cylindrical shell can be obtained.

4.2. Free vibration of a submerged cylindrical shell

Due to the coupling effect between the fluid medium and the shell, the vibration of submerged shells are different from the vibration of shells in vacuum. The free vibration of a cylindrical shell submerged in an infinite incompressible fluid medium is considered in this paper. The basic equation of the dynamic pressure $P(z, \theta, r, t)$ in cylindrical coordinates (z, θ, r) is given by:

$$\frac{\partial^2 P}{\partial z^2} + \frac{1}{r}\frac{\partial}{\partial r}\left(r\frac{\partial P}{\partial r}\right) + \frac{1}{r^2}\frac{\partial^2 P}{\partial \theta^2} = 0 \tag{40}$$

The boundary conditions on the interaction surface of the fluid and the shell $(r = R)$ are:

$$\frac{\partial P}{\partial r} = -\rho_{\mathrm{f}} \frac{\partial^2 u_{\mathrm{r}}}{\partial t^2}, \quad \sigma_{\mathrm{r}} = -P \tag{41}$$

where ρ_{f} is the fluid density, and u_{r} and σ_{r} are the radial displacement and stress components of the shell on the interaction surface, respectively. Therefore, $u_{\mathrm{r}} = u_3$ and $P_1(x_1, x_2, t) = P(z, \theta, r, t)|_{r=R}$.

Dynamic pressure $P(z, \theta, r, t)$ can be expanded in the following form:

$$P(z, \theta, r, t) = P_{mn} X(r) \sin(z_m z) \cos(n\theta) \mathrm{e}^{\mathrm{i}\omega t} \tag{42}$$

Substituting Eq. (42) into Eq. (40) yields

$$\frac{\mathrm{d}^2 X}{\mathrm{d}r^2} + \frac{1}{r}\frac{\mathrm{d}X}{\mathrm{d}r} - \left(z_m^2 + \frac{n^2}{r^2}\right) X = 0 \tag{43}$$

Taking account of the non-reflection condition of P at $r = \infty$, the solution of Eq. (43) is:

$$X(r) = K_n(vr) \tag{44}$$

where $v = z_m$, and $K_n(r)$ is the second kind of Bessel function of order n.

From Eqs. (41) and (36), we can obtain

$$P(z, \theta, r, t) = \omega^2 \rho_{\mathrm{f}} w_{mn} \frac{X(r)}{X'(R)} \sin(z_m z) \cos(n\theta) \mathrm{e}^{\mathrm{i}\omega t} \tag{45}$$

where

$$X'(r) = \frac{\mathrm{d}X(r)}{\mathrm{d}r}$$

Comparing Eq. (45) with Eq. (37), we obtain

$$P_{1\,mn} = \omega^2 \rho_{\mathrm{f}} w_{mn} \frac{X(R)}{X'(R)} \tag{46}$$

Substituting Eq. (46) into Eq. (38) yields the frequency equation of the submerged piezoelastic shell as

$$([H] - sq_{\mathrm{cr}}[J])\{V\} = \omega^2([M] + [M_a])\{V\} \tag{47}$$

where $[M_a]$ is a diagonal matrix, whose elements are

$$M_{a33} = -\rho_{\mathrm{f}} \frac{X(R)}{X'(R)}, \qquad M_{aii} = 0 \quad (i = 1, 2, 4, 5)$$

Comparing Eq. (47) with Eq. (39), it can be seen that the effect of the fluid–structural coupling is included in the matrix $[M_a]$.

5. Numerical examples

Numerical examples are shown in this section. The hybrid laminate is a six-layer hybrid laminate with two piezoelastic layers of the same piezoelectric material integrated symmetrically to a four-layer graphite/epoxy substrate, which is symmetric cross-ply with ply angles $[0°/90°]_s$, and ply thickness t_{g}. Let t_{p} denote the piezoelastic layer thickness. It is supposed that the length L and the radius R of the cylindrical shell are 10.0 and 1.0 m, respectively. Material properties of graphite/epoxy are

$$E_1 = 181.0\ \text{GPa}, \quad E_2 = E_3 = 10.3\ \text{GPa}, \quad G_{12} = G_{13} = 7.17\ \text{GPa}, \quad G_{23} = 3.87\ \text{GPa},$$
$$v_{12} = v_{13} = 0.28, \quad v_{23} = 0.33, \quad \rho = 1580.0\ \text{kg/m}^3$$

Table 1
Elastic, piezoelectric and dielectric properties of piezoelectric materials

Property	PVDF	PZT
C_{11} (GPa)	3.61	148
C_{22}	3.13	148
C_{33}	1.63	131
C_{12}	1.61	76.2
C_{13}	1.42	74.2
C_{23}	1.31	74.2
C_{44}	0.55	25.4
C_{55}	0.59	25.4
C_{66}	0.69	35.9
e_{31} (C/m^2)	32.075×10^{-3}	−2.1
e_{32}	-4.07×10^{-3}	−2.1
e_{33}	-21.19×10^{-3}	9.5
e_{15}	-15.93×10^{-3}	9.2
e_{24}	-12.65×10^{-3}	9.2
$\varepsilon_{11}/\varepsilon_0$ [a]	6.1	460
$\varepsilon_{22}/\varepsilon_0$ [a]	7.5	460
$\varepsilon_{33}/\varepsilon_0$ [a]	6.7	235
ρ (kg/m^3)	1800	7600

[a] $\varepsilon_0 = 8.85 \times 10^{-12}$ C^2/Nm^2.

The material properties of piezoelectric laminae are listed in Table 1. The density of the fluid ρ_f is 1000.0 kg/m^3.

Because the lowest natural frequency of the structure is more important than other higher ones in engineering, the frequencies calculated in this section are the lowest frequencies of the shell. The lowest natural frequencies of the piezoelastic cylindrical shell in vacuum and in a fluid under different hydrostatic external pressures are listed in Table 2, where PVDF are chosen for the piezoelastic layers in calculations. It can be seen that, for a given vibration mode, the natural frequencies of the shell decrease when the hydrostatic external pressure increases. When the hydrostatic pressure reaches the critical pressure, the shell will lose its stability. Also, the frequencies of a submerged shell are less than half of those of the shell in vacuum under the same hydrostatic pressure, which means that the fluid–structural coupling effect has great impact on the frequencies of submerged shells.

Fig. 2(a) and (b) give the curves of critical hydrostatic pressure and the frequency of the laminated piezoelastic cylindrical shell versus various values of m and n, respectively, where the piezoelectric pairs are PVDF. The results of the Fig. 2 were obtained with $t_g = 0.01$ m and $t_p = 0.001$ m. When the total thickness of the shell is set constant, i.e. $h = 0.042$ m, the critical hydrostatic pressure and the frequency of the laminated piezoelastic cylindrical shell for different ratios $2t_p/h$ are shown in Fig. 3 for PVDF pairs and Fig. 4 for PZT pairs. In Figs. 2–4(b), the solid lines represent the cases without considering the fluid–structural coupling effect and the dashed lines represent the cases considering the fluid–structural coupling effect.

As indicated in Fig. 2, for a given axial half-waves number m, q_{cr} and natural frequency decrease first and rise later with the increase of the circumferential wave number. For a given circumferential wave number n, q_{cr} and natural frequency increase with the increase of the axial half-waves number m.

If the thickness of the shell is set constant, when the PVDF laminae become thicker, the stiffness of the shell reduces and the critical hydrostatic pressure reduces. However, because the density of PVDF is close to that of graphite/epoxy, when the piezoelectric thickness ratio increases, the mass of the shell changes little and the natural frequencies of the shell decrease (see Fig. 3). The results are different for the laminae containing PZT laminae. PZT is mechanically stronger than graphite/epoxy, and the stiffness of the shell

Table 2
Comparison of the natural frequencies of the piezoelastic cylindrical shell in vacuum and in a fluid under different hydrostatic external pressures (PVDF pairs)

t_g/t_p		Mode		Natural frequency ω (rad/s)					q_{cr} (10^6 N/m^2)
		m	n	$s=0$	$s=0.2$	$s=0.4$	$s=0.6$	$s=0.8$	
10	In vacuum	1	3	393.7395	352.1725	304.9914	249.0252	176.0880	1.2728
	In a fluid			168.6531	150.8479	130.6381	106.6656	75.4240	
	In vacuum	3	4	826.2558	739.0295	640.0217	522.5782	369.5205	2.9499
	In a fluid			394.0439	352.4437	305.2252	249.2154	176.2220	
1	In vacuum	1	3	245.3848	219.4792	190.0750	155.1959	109.7403	0.5139
	In a fluid			106.7760	95.5034	82.7084	67.5311	47.7517	
	In vacuum	3	4	536.8807	480.2023	415.8687	339.5565	240.1035	1.2947
	In a fluid			259.8825	232.4460	201.3042	164.3642	116.2231	
0.5	In vacuum	1	3	179.5319	160.5784	139.0652	113.5464	80.2895	0.2812
	In a fluid			78.8169	70.4960	61.0514	49.8482	35.2480	
	In vacuum	3	4	407.3876	364.3795	315.5627	257.6565	182.1911	0.7619
	In a fluid			198.8598	177.8656	154.0362	125.7700	88.9329	

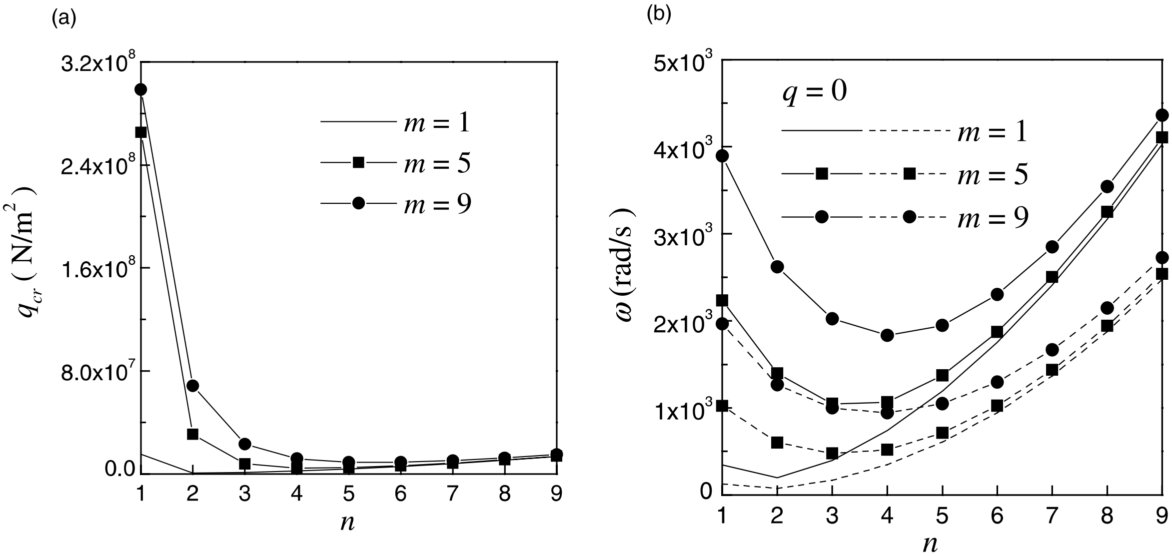

Fig. 2. (a) The critical hydrostatic pressure q_{cr}; (b) the natural frequency of the piezoelastic cylindrical shell without considering hydrostatic pressure for various values of m and n ($t_g = 0.01$ m and $t_p = 0.001$ m, PVDF pairs).

increases when the PZT layers become thicker. Hence, the critical hydrostatic pressure increases. Moreover, because the density of PZT is greater than that of graphite/epoxy, as the piezoelectric thickness ratio increases, the effect of mass increase is greater than that of stiffness increase. Hence, the natural frequencies increase first and then decrease (see Fig. 4).

The natural frequency of the shell is lower when the fluid–structural coupling effect is considered, as indicated in Figs. 2–4(b). It means that the fluid–structural coupling effect is similar to adding mass.

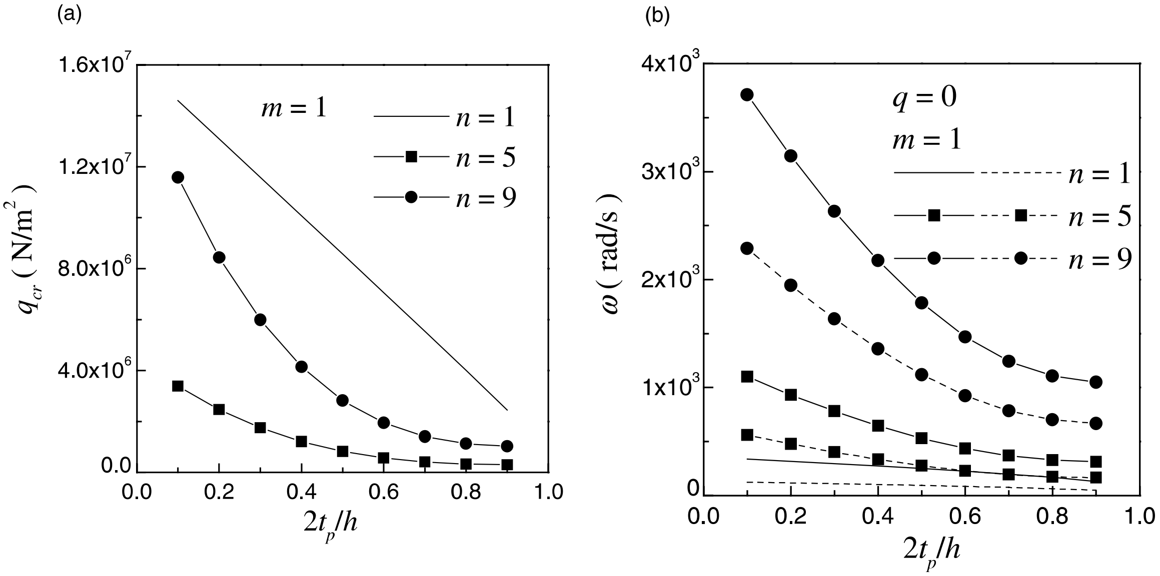

Fig. 3. (a) The critical hydrostatic pressure q_{cr}; (b) the natural frequency of the piezoelastic cylindrical shell versus piezoelectric thickness ratio ($h = 0.042$ m, PVDF pairs).

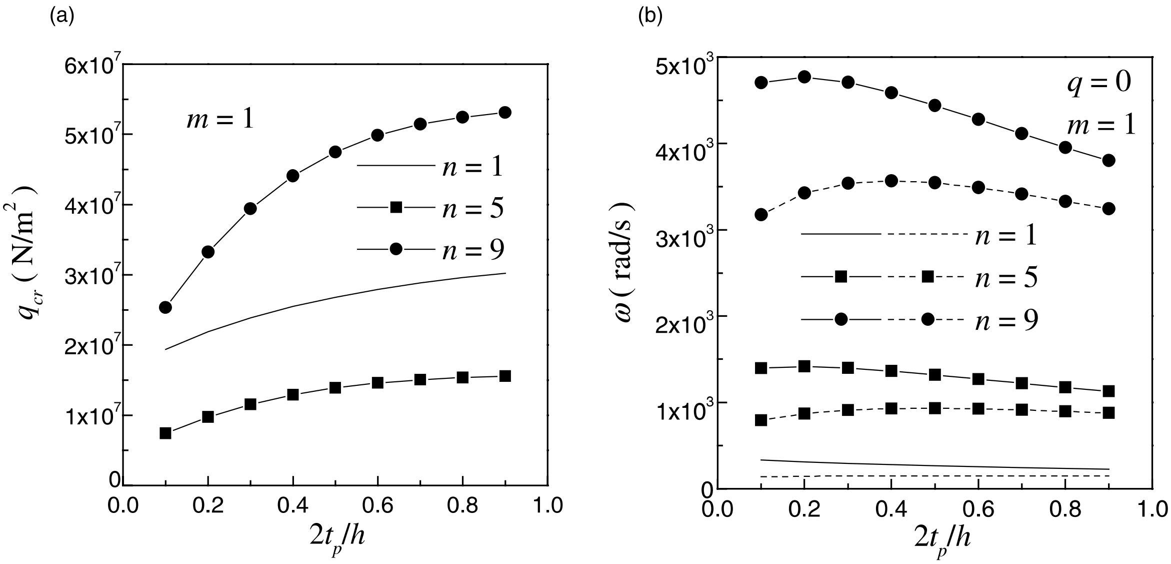

Fig. 4. (a) The critical hydrostatic pressure q_{cr}; (b) the natural frequency of the piezoelastic cylindrical shell versus piezoelectric thickness ratio ($h = 0.042$ m, PZT pairs).

6. Conclusion

Free vibration of piezoelastic laminated cylindrical shells under a hydrostatic pressure is investigated in this paper. The nonlinear dynamic equations of a closed piezoelastic cylindrical shell under a hydrostatic external pressure are obtained. For the case of simply supported piezoelastic laminated cylindrical shell under a hydrostatic pressure, solutions of the critical hydrostatic pressure and the natural frequencies of the shell in vacuum and in a fluid are presented. The results show that: (1) the critical hydrostatic pressure and the natural frequencies of piezoelastic laminated shells are determined not only by the stiffness and mass of the structures, but also by the piezoelectric and dielectric constants of piezoelectric layers; (2) the natural frequencies of the piezoelastic cylindrical shell decrease with the increase of the hydrostatic pressure; (3) the fluid–structural coupling effect is significant to natural frequencies of submerged shells, which is similar to adding mass.

Acknowledgements

The supports of this work from the National Defense's Technical Application and Research Foundation of Chinese marine industry (no. 99J41.4.4) and the Open Foundation of the National Key Laboratory of Vibration, Sound and Noise of China (no. VSN-99001) are greatly appreciated.

References

Bao, Y., Tzou, H.S., Venkayya, V.B., 1998. Analysis of nonlinear piezothermoelastic laminated beams with electric and temperature effects. J. Sound Vib. 209 (3), 505–518.

Baumhauer, J.C., Tiersten, H.F., 1973. Nonlinear electroelastic equations for small fields superposed on a bias. J. Acoust. Soc. Am. 54 (4), 1017–1033.

Cheng, C.Q., Shen, Y.P., 1997. Stability analysis of piezoelectric circular cylindrical shells. J. Appl. Mech. 64 (4), 847–852.

Clinton, Y.K., Li, Y.T., Grant, P.S., 1998. A review on the modeling of piezoelectric sensors and actuators incorporated in intelligent structures. J. Intel. Mater. Syst. Struct. 9 (1), 3–19.

Donatus, C.D.G., Sergio, F., Jorn, S.H., 1998. Stress stiffening effects in laminated beams with piezoelectric actuators. J. Intel. Mater. Syst. Struct. 9 (2), 137–145.

Lee, C.K., 1990. Theory of laminated piezoelectric plates for the design of the design of distributed sensors/actuators: part I: governing equations and reciprocal relationships. J. Acoust. Soc. Am. 87 (3), 1144–1158.

Mitchell, J.A., Reddy, J.N., 1995. A refined hybrid plate theory for composite laminates with piezoelectric laminae. Int. J. Solids Struct. 32 (16), 2345–2367.

Pai, P.F., Nafeh, A.H., Mook, D.T., 1993. A refined nonlinear model of piezoelectric plate with integrated piezoelectric actuators and sensors. Int. J. Solids Struct. 30 (11), 1603–1630.

Palazatto, A.N., Dennis, S.T., 1992. Nonlinear Analysis of Shell Structures. AIAA Publisher, Washington, DC.

Tiersten, H.F., 1969. Linear Piezoelectric Plate Vibrations. Plenum Press, New York.

Tzou, H.S., 1993. Piezoelectric Shells (Distributed Sensing and Control of Continua). Kluwer, Dordrecht.

Tzou, H.S., Bao, Y., 1997. Nonlinear piezothermoelasticity and multi-field actuations, part 1: nonlinear anisotropic piezothermoelastic shell laminates. J. Vib. Acoust. 119 (3), 374–381.

Tzou, H.S., Zhong, J.P., Natori, M., 1993. Sensor mechanics of distributed shell convolving sensors applied to flexible rings. J. Vib. Acoust. 115 (1), 40–46.

Tzou, H.S., Zhou, Y.H., 1995. Dynamics and control of nonlinear circular plates with piezoelectric actuators. J. Sound Vib. 188 (2), 189–207.

Yu, Y.Y., 1995. On the ordinary, generalized, and pseudo-variational equations of motion in nonlinear elasticity, piezoelectricity and classical plate theories. J. Appl. Mech. 62 (2), 471–478.

Hongyun Li received the B.S. degree and the Ph.D. degree in Engineering Mechanics from Shanghai Jiaotong University, People's Republic of China, in 1993 and 1998, respectively. In 1998, she joined the faculty of the Department of Engineering Mechanics, Shanghai Jiaotong University. Her research interests have been in mechanical analysis of intelligent structures and their applications, and computational mechanics.